ANALYSIS OF A GRADIENT TRANSPORT MODEL FOR TURBULENT DENSITY-STRATIFIED SHEAR FLOW

Communications on Hydraulics

Report No. 80-2

C.Kranenburg

Laboratory of Fluid Mechanics
Department of Civil Engineering
Delft University of Technology

1980

An earlier version of section 2 was published by Kranenburg (1980).

ABSTRACT

A number of qualitative properties of a first-order gradient transport model for turbulent density-stratified flow is analyzed. The dynamical stability of a statically stable shear flow is considered to re-examine certain arguments found in the literature which are in favour of the possibility of instability. Real flows seem to be stable in the sense that in homogeneous turbulence sharp interfaces do not arise spontaneously. Furthermore the development of an interface between two homogeneous layers is dealt with, and is found to be in line with the stability analysis and with experimental evidence reported in the literature.

Report No. 80-2

The following reference should be added:

Linden, P.F., 1979: Mixing in stratified fluids, *Geophys. Astrophys. Fluid Dyn.*, 13, 3-23.

CONTENTS page

1. INTRODUCTION

Despite the rapid development of various higher-order turbulence closure schemes of recent years, relatively simple gradient transport models continue to be a useful tool for the computation of nearly horizontal flows in which the turbulence is influenced by density stratification. In these models the vertical transports of momentum and buoyancy are assumed proportional to the vertical gradients of mean horizontal velocity and mean buoyancy. It is common practice to write the proportionality coefficients - eddy viscosity and eddy diffusivity - as products of turbulence velocity and length scales, both under neutral conditions, and a function of a local (gradient) Richardson number to account for the damping effects of buoyancy.

A number of qualitative properties of a model of this type is analyzed in this report. In section 2 the dynamical stability of a statically stable shear flow (Couette flow) is considered to critically re-examine certain arguments found in the literature which are in favour of the possibility of instability. Section 3 deals with the development of an interface between two homogeneous layers. The results of this section are compared with those of section 2 and with experimental evidence reported in the literature.

2. STABILITY OF TURBULENT, STRATIFIED SHEAR FLOW

2.1. Formulation of the problem

It is sometimes argued (Phillips, 1972; Posmentier, 1977) that a turbulent density-stratified shear flow may become unstable because an effective eddy diffusivity relating to the vertical buoyancy transport (caused by differences in salinity or temperature, for instance) would become negative under strongly stratified conditions. Both Phillips and Posmentier ignore the interaction between buoyancy field and velocity field, and find that finestructure may develop when the buoyancy field is dynamically unstable. The purpose of the present analysis is to examine the influence of the interaction between both fields on the stability of the flow. The approaches of Phillips and Posmentier are included as special cases.

Consider a horizontally homogeneous shear flow (turbulent Couette flow) in which the vertical turbulent transport may be modelled as gradient transports. The mean horizontal momentum and buoyancy equations then are

$$\frac{\partial \bar{u}}{\partial t} = \frac{\partial}{\partial z} \left(K_m \frac{\partial \bar{u}}{\partial z} \right) \tag{2.1}$$

$$\frac{\partial \bar{b}}{\partial t} = \frac{\partial}{\partial z} \left(K_b \frac{\partial \bar{b}}{\partial z} \right) \tag{2.2}$$

where $\bar{u}$ is the mean horizontal velocity, $\bar{b} = -g\delta\bar{\rho}/\rho_r$ the mean buoyancy, ρ_r a reference density, $\delta\bar{\rho}$ the deviation from ρ_r, g the acceleration due to gravity, z the vertical co-ordinate, t time, and K_m and K_b are the eddy viscosity and eddy diffusivity.

Regarding the dependence of K_m and K_b on the stratification, two cases will be considered, namely a case where the vertical length scale of the energy containing eddies is determined by

geometrical constraints (wall-affected turbulence, case I), and a case where this length scale is determined by the density stratification (free turbulence, case II). Case I resembles that considered by Posmentier, case II is that analyzed by Phillips.

The assumed expressions are for case I

$$K_m = u_* l_n F(Ri) \tag{2.3}$$

$$K_b = u_* l_n G(Ri) \tag{2.4}$$

and for case II (see Phillips)

$$K_m = u_*^2 N^{-1} F(Ri) \tag{2.5}$$

$$K_b = u_*^2 N^{-1} G(Ri) \tag{2.6}$$

Here u_* is a friction velocity, l_n a mixing length under neutral conditions, $N = (\partial\bar{b}/\partial z)^{1/2}$ the local buoyancy frequency, and F and G are functions representing the influence of the stability of the flow as characterized by the local gradient Richardson number Ri ($Ri \geq 0$),

$$Ri = \frac{\partial\bar{b}}{\partial z} \left(\frac{\partial\bar{u}}{\partial z}\right)^{-2} \tag{2.7}$$

The functions F and G are positive and decrease as Ri increases (dF/dRi and $dG/dRi < 0$). Explicit expressions for F and G will not be given here, since these functions are different to determine experimentally and moreover may differ somewhat from one situation to another.

2.2. Linear stability analysis

The undisturbed buoyancy and velocity profiles are assumed to be

time-independent and (locally) linear functions of z; the turbulence is (locally) homogeneous and stationary. Infinitesimal perturbations $\alpha u(z,t)$ and $\beta b(z,t)$ are introduced according to

$$\bar{u}(z,t) = U_o + \alpha z + \alpha u(z,t) \tag{2.8}$$

$$\bar{b}(z,t) = B_o + \beta z + \beta b(z,t) \tag{2.9}$$

where U_o, B_o, α and β are constants ($\beta \geq 0$); the coefficients α and β multiplying u and b have been introduced for the sake of convenience. A possible dependence of the perturbations on a horizontal coordinate is not considered.

Substituting (2.8) and (2.9) into (2.1), (2.2) and (2.7), and linearizing yield as perturbation equations

$$\frac{\partial u}{\partial t} = K_{11} \frac{\partial^2 u}{\partial z^2} + K_{12} \frac{\partial^2 b}{\partial z^2} \tag{2.10}$$

$$\frac{\partial b}{\partial t} = K_{21} \frac{\partial^2 u}{\partial z^2} + K_{22} \frac{\partial^2 b}{\partial z^2} \tag{2.11}$$

where for case I (using (2.3) and (2.4))

$$[K] = u_* l_n \begin{bmatrix} (F - 2Ri\ F')_o & (Ri\ F')_o \\ -(2Ri\ G')_o & (G + Ri\ G')_o \end{bmatrix} \tag{2.12}$$

and for case II (using (2.5) and (2.6))

$$[K] = u_*^2 N_o^{-1} \begin{bmatrix} (F - 2Ri\ F')_o & -(\frac{1}{2} F - Ri\ F')_o \\ -(2Ri\ G')_o & (\frac{1}{2} G + Ri\ G')_o \end{bmatrix} \tag{2.13}$$

Here subscript o denotes the undisturbed situation, $Ri = Ri_o = \beta/\alpha^2$ and $N_o = \beta^{1/2}$. A prime denotes differentiation with respect to Ri.

Eqs. 2.10 and 2.11 show a linear interaction between buoyancy field and velocity field.

A harmonic solution to (2.10) and (2.11) can be obtained in the usual way by letting

$$u = \hat{u} \exp(\lambda t + ikz) \tag{2.14}$$

$$b = \hat{b} \exp(\lambda t + ikz) \tag{2.15}$$

where k is a real wave number, λ a (possibly complex) frequency, and $\hat{u}$ and $\hat{b}$ are constants. Stable solutions are obtained if $\mathrm{Re}\,\lambda \leq 0$, whereas $\mathrm{Re}\,\lambda > 0$ implies instability of the system. Substituting (2.14) and (2.15) into the governing equations, two homogeneous, algebraic equations in $\hat{u}$ and $\hat{b}$ are obtained. In order that these (linear) equations be compatible the coefficient determinant must vanish. Thus one arrives at a quadratic equation,

$$\left(\frac{\lambda}{k^2}\right)^2 + (K_{11} + K_{22})\left(\frac{\lambda}{k^2}\right) + (K_{11}K_{22} - K_{12}K_{21}) = 0 \tag{2.16}$$

In (2.16) the wave number k figures in the quotient λ/k^2 only. Therefore, the stability boundary ($\mathrm{Re}\,\lambda = 0$), if any, does not depend on k.

The conditions for stability ($\mathrm{Re}\,\lambda \leq 0$) following from (2.16) are

$$K_{11} + K_{22} \geq 0 \tag{2.17}$$

and

$$K_{11}K_{22} - K_{12}K_{21} \geq 0 \tag{2.18}$$

A simple physical analogy exists to illustrate these results. Eliminating u, for instance, between (2.10) and (2.11) gives

$$\frac{\partial^2 b}{\partial t^2} - (K_{11} + K_{22}) \frac{\partial^3 b}{\partial z^2 \partial t} + (K_{11}K_{22} - K_{12}K_{21}) \frac{\partial^4 b}{\partial z^4} = 0 \qquad (2.19)$$

This equation describes the transverse oscillations of an elastic bar. If b represents the transverse displacement of a material element of the bar, the second term of (2.19) is proportional to the rate of strain. It is a damping term provided (2.17) is satisfied. Eq. 2.18 is equivalent of the condition that the modulus of elasticity (Young's modulus) be nonnegative.

Returning to the problem under consideration, the two cases I and II are now discussed separately.

case I

Using (2.12) conditions (2.17) and (2.18) may be written as (the subscript o is dropped)

$$F \left[1 + \frac{d}{dRi} \left(\frac{G}{F} Ri\right)\right] + \left(2 - \frac{G}{F}\right)(-RiF') \geq 0 \qquad (2.20)$$

$$\frac{d}{dRi} \left(\frac{G}{F^2} Ri\right) \geq 0 \qquad (2.21)$$

The ratio $F/G = Pr_t$ is known as the turbulent Prandtl (or Schmidt) number. Experimental evidence shows that under neutral conditions $F/G \simeq 0.5$ in plane jets and mixing layers, somewhat larger in other free flows, and certainly larger in near-wall flows. Furthermore, F/G increases with stability in free flows (e.g. Townsend, 1976, p. 374; Turner, 1973, p. 161; Webster 1964). For stratified shear flow it may therefore be assumed that

$$Pr_t > 0.5 \qquad (2.22)$$

Measurements also indicate that the expression (G/F)Ri increases with Ri (additional references: Arya, 1972; Gartrell, 1979). On the assumption of gradient transport it is equal to the flux Rirchardson number (e.g. Turner, 1973, p. 133), which number is found to increase with Ri in shear flow, also see McEwan (1980). It may therefore be concluded that

$$\frac{d}{dRi}\left(\frac{G}{F}\,Ri\right) > 0 \qquad (2.23)$$

The experimental results (2.22) and (2.23) indicate that both (2.20) and (2.21) are satisfied ($2 - G/F = 2 - Pr_t^{-1} > 0$, $F' < 0$, $(G/F^2)Ri = ((G/F)Ri)/F$). Consequently, the flow will be stable.

Posmentier (1977) ignored the perturbation of the velocity field, implicitly assuming that F (or K_m) does not depend on Ri. Eq. 2.17 then becomes $K_{22} \geq 0$ indicating that instability would occur when $K_{22} = G + RiG' = d(Ri\ G)/dRi < 0$. Walters, Carey and Winter (1978) also arrive at this conclusion, but state that the unstable case is not an acceptable one. Condition 2.18 does not arise in Posmentier's analysis. The differences from the results obtained here demonstrate that the dependence of F on Ri must not be ignored, although in certain cases this dependence may be weaker than that of G on Ri.

case II

Using (2.13) conditions (2.17) and (2.18) may be written as

$$F\,\frac{d}{dRi}\left(\frac{G}{F}\,Ri\right) + \left(2 - \frac{G}{F}\right)\left(\frac{1}{2}\,F - Ri\,F'\right) \geq 0 \qquad (2.24)$$

$$\left(\frac{1}{2} - Ri\,F'\right)G \geq 0 \qquad (2.25)$$

Condition (2.25) is always satisfied ($F' < 0$), and (2.22) and (2.23) indicate that (2.24) is also satisfied. Again it may be concluded that the flow is stable.

Phillips (1972) also considered the behaviour of K_{22} only. In case II K_{22} is given by

$$K_{22} = \frac{1}{2} G + Ri\ G' = Ri^{\frac{1}{2}} \frac{d}{dRi} (Ri^{\frac{1}{2}} G) \qquad (2.26)$$

Phillips based his instability argument on the behaviour of the expression $d(Ri^{\frac{1}{2}}G)/dRi$.

2.3. Discussion

Summarizing it can be concluded that taking into account the interaction between buoyancy field and velocity field through the gradient Richardson number will lead to stable solutions, since (2.22) and (2.23) are likely to be satisfied in real shear flows. Therefore, the mathematical model represented by Eq. 2.1 through 2.7 does not predict finestructure, or a system of sheets and layers, in initially homogeneous turbulence.

The dependent variables in the mathematical model are ensemble-averaged quantities so far as turbulence is concerned. Since turbulence itself is an instability phenomenon, the length scale of any instability produced by the model must be larger, at least by an order of magnitude, than that of the turbulence. Eq. 2.16 shows, however, that a possible instability does not depend on the scale ($=k^{-1}$), that is, if the flow is unstable it is unstable at all scales (in fact, the small scale disturbances then grow most rapidly). If this point of view is correct, only such functions F(Ri) and G(Ri) would be admissable that the stability conditions 2.17 and 2.18 are satisfied.

It must be kept in mind that the question under what conditions the gradient transport model adequately describes the physics underlying it has not been considered.

3. DEVELOPMENT OF THE INTERFACE BETWEEN TWO HOMOGENEOUS LAYERS

3.1. Problem considered

In section 2 the behaviour of small perturbations on a steady-state situation, in which the profiles of both mean velocity $\bar{u}$ and mean buoyancy $\bar{b}$ were linear, was analyzed. In this section a somewhat different problem is considered, namely the development of an interface or mixing layer between two homogeneous layers in a plane Couette flow, see Fig. 3.1. The flow at the interface is assumed to be turbulent. The homogeneous layers may be laminar or weakly turbulent so that the turbulence at the interface is internally generated. The overall Richardson number $\Delta b\, h/\Delta u^2$ is assumed to be sufficiently large so that the thickness of the interface remains less than the height, 2h, of the channel. Here $2\Delta b$ and $2\Delta u$ are the imposed differences in mean buoyancy and velocity between top and bottom of the channel.

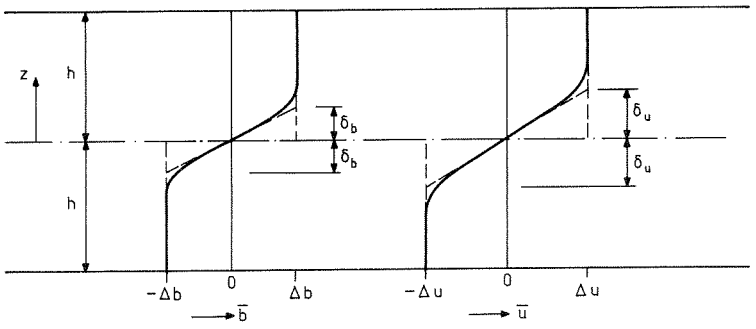

Fig. 3.1 - Definition sketch of stratified Couette flow.

In section 3.2 the evolution of the maximum-slope thicknesses $2\delta_b$ and $2\delta_u$ of the buoyancy and velocity profiles, respectively, is examined on the basis of Eqs. 2.1, 2.2, 2.3, 2.4 and 2.7 (case I of section 2). An increasing thickness of the interface would indicate diffusive behaviour corresponding with the stable solutions

discussed in section 2, whereas a decrease in thickness would lead to the formation of a sharp interface also arising in the unstable solutions obtained by Posmentier (1977). The results of this section need not necessarily be identical to those of section 2, since the initial buoyancy and velocity profiles are different and the perturbations are finite.

Experiments relating to the problem considered are described by Thorpe (1971, 1973) and Gartrell (1979), for instance. Also see the review paper of Sherman, Imberger and Corcos (1978). These experiments reveal that the Kelvin-Helmholtz instability of an initially sharp interface between two homogeneous layers causes the rolling up of the vortex sheet at the interface to form billows. The subsequent breaking of the billows produces turbulence and thickening of the interface. If no turbulence is generated externally (at a bottom, for instance), the turbulence at the thickened interface collapses after a certain time interval, and a laminar flow remains.

Of course, the mathematical model employed cannot reproduce the billow structure of the flow. At best it can predict the mean-flow quantities $\bar{u}$, $\bar{b}$, and transports of buoyancy and momentum as functions of position (z) and time.

3.2. Evolution of interface thicknesses δ_u and δ_b

It is assumed that the mixing length, l_n, for homogeneous flow in (2.3) and (2.4) is proportional to the (time-dependent) thickness of the interface* and does not depend on z. A possible inhomogeneity of

---

* The case where l_n is proportional to the height, 2h, of the channel gives similar results, and would apply to externally generated turbulence.

the turbulence is thus caused by the stratification through the functions F(Ri) and G(Ri). Experimental evidence indicates that in general δ_u and δ_b are different. The mixing length l_n is, rather arbitrarily, assumed proportional to δ_u. The shear flow velocity u_* is taken to be proportional to Δu. Eqs. 2.1 to 2.4 then become

$$\frac{\partial \bar{u}}{\partial t} = k\, \Delta u\, \delta_u \frac{\partial}{\partial z}\left[F(Ri)\, \frac{\partial \bar{u}}{\partial z}\right] \tag{3.1}$$

$$\frac{\partial \bar{b}}{\partial t} = k\, \Delta u\, \delta_u \frac{\partial}{\partial z}\left[G(Ri)\, \frac{\partial \bar{b}}{\partial z}\right] \tag{3.2}$$

where k is a proportionality constant. It seems reasonable to assume that the $\bar{u}$ and $\bar{b}$ profiles are antisymmetric and of similar shape when scaled with δ_u and δ_b, respectively. Therefore, the following Taylor series expansions with respect to z=0 are attempted:

$$\bar{u} = \Delta u \left[\frac{z}{\delta_u} - \frac{\phi}{6}\left(\frac{z}{\delta_u}\right)^3 + \ldots\right] \tag{3.3}$$

$$\bar{b} = \Delta b \left[\frac{z}{\delta_b} - \frac{\phi}{6}\left(\frac{z}{\delta_b}\right)^3 + \ldots\right] \tag{3.4}$$

where ϕ is an unknown factor ($\phi > 0$), which may be a function of time. The measurements of Gartrell (1979) suggest that both velocity and buoyancy profiles are self-similar at all instants*. In that case ϕ is a positive constant.

Substituting (3.3) and (3.4) into (2.7) gives the gradient Richardson number, Ri, as

$$Ri = Ri_o \left[1 + \frac{1}{2}\phi z^2 \left(\frac{2}{\delta_u^2} - \frac{1}{\delta_b^2}\right) + \ldots\right] \tag{3.5}$$

where Ri_o is the value of Ri at z=0,

---

* Owing to the upstream boundary conditions the profiles observed by Gartrell were not exactly antisymmetric.

$$Ri_o = \frac{\Delta b \, \delta_u^2}{\Delta u^2 \delta_b} \tag{3.6}$$

Eq. 3.5 shows that Ri is maximal at z=0 if $\delta_u > \delta_b\sqrt{2}$, and minimal if $\delta_u < \delta_b\sqrt{2}$. Substituting (3.3), (3.4) and (3.5) into the governing equations 3.1 and 3.2 gives

$$\frac{1}{\delta_u^2}\frac{d\delta_u}{dt} z + k \, \Delta u \, \delta_u \frac{\partial}{\partial z} \left\{ \left[F_o + \frac{1}{2}\phi z^2 \left(\frac{2}{\delta_u^2} - \frac{1}{\delta_b^2}\right) F_o' \, Ri_o \right] \times \left(\frac{1}{\delta_u} - \frac{1}{2}\phi \frac{z^2}{\delta_u^3}\right) \right\} + \ldots = 0$$

$$\frac{1}{\delta_b^2}\frac{d\delta_b}{dt} z + k \, \Delta u \, \delta_u \frac{\partial}{\partial z} \left\{ \left[G_o + \frac{1}{2}\phi z^2 \left(\frac{2}{\delta_u^2} - \frac{1}{\delta_b^2}\right) G_o' \, Ri_o \right] \times \left(\frac{1}{\delta_b} - \frac{1}{2}\phi \frac{z^2}{\delta_b^3}\right) \right\} + \ldots = 0$$

where $F' = dF/dRi$ and $F_o = F(Ri_o)$. Similar definitions apply to function G. Equating in both equations the coefficient of z to zero yields

$$\frac{1}{k \, \Delta u \, \delta_u^2 \, \phi}\frac{d\delta_u}{dt} + F_o' \, Ri_o \left(\frac{2}{\delta_u^2} - \frac{1}{\delta_b^2}\right) - \frac{F_o}{\delta_u^2} = 0 \tag{3.7}$$

$$\frac{1}{k \, \Delta u \, \delta_u \, \delta_b \, \phi}\frac{d\delta_b}{dt} + G_o' \, Ri_o \left(\frac{2}{\delta_u^2} - \frac{1}{\delta_b^2}\right) - \frac{G_o}{\delta_b^2} = 0 \tag{3.8}$$

The unknown function $\phi = \phi(t)$ may be absorbed in the time variable by introducing a new time variable, t_1, according to

$$t_1 = \int_0^t \phi(t')\, dt' \tag{3.9}$$

The time variable t_1 increases as t increases, since ϕ is positive. Eqs. 3.7 and 3.8 then become

$$\frac{1}{k\,\Delta u\,\delta_u^2}\frac{d\delta_u}{dt_1} + F_o' Ri_o \left(\frac{2}{\delta_u^2} - \frac{1}{\delta_b^2}\right) - \frac{F_o}{\delta_u^2} = 0 \tag{3.10}$$

$$\frac{1}{k\,\Delta u\,\delta_u\delta_b}\frac{d\delta_b}{dt_1} + G_o' Ri_o \left(\frac{2}{\delta_u^2} - \frac{1}{\delta_b^2}\right) - \frac{G_o}{\delta_b^2} = 0 \tag{3.11}$$

Introducing dimensionless variables y, x and τ according to

$$\begin{aligned} \delta_u &= y(\Delta u^2/\Delta b) \\ \delta_b &= x(\Delta u^2/\Delta b) \\ t_1 &= \tau(\Delta u/(k\Delta b) \end{aligned} \tag{3.12}$$

changes (3.6), (3.10) and (3.11) to the following second-order system for the dimensionless interface thicknesses y and x as functions of dimensionless time τ (the subscript o is dropped)

$$\frac{\dot{y}}{y^2} + F'Ri\left(\frac{2}{y^2} - \frac{1}{x^2}\right) - \frac{F}{y^2} = 0 \tag{3.13}$$

$$\frac{\dot{x}}{xy} + G'Ri\left(\frac{2}{y^2} - \frac{1}{x^2}\right) - \frac{G}{x^2} = 0 \tag{3.14}$$

$$Ri = \frac{y^2}{x} \tag{3.15}$$

where $\dot{y} = dy/d\tau$ and $\dot{x} = dx/d\tau$.

Eqs. 3.13 to 3.15 could be integrated, in general numerically, if explicit expressions for the functions F and G, and initial conditions (y(0) and x(0)) are given. For the present purpose, namely to answer the question whether a sharp interface can develop, numerical integration is not necessary. Instead, the equations are examined analytically in the Appendix to obtain an understanding of the behaviour of the solutions to (3.13) to (3.15).

Regarding the functions F and G the inequalities 2.22 and 2.23 are adopted. Furthermore the assumption is made that a critical Richardson number, Ri_c, exists beyond which turbulence disappears so that F and G then vanish,

$$F = G = 0 \quad \text{if} \quad Ri \geq Ri_c \tag{3.16}$$

The results are conveniently presented in a phase plane (x,y-plane) by conceiving of the functions $y = y(\tau)$ and $x = x(\tau)$ as a parameter representation (with the time variable τ as a parameter) of y as a function of x. Fig. 3.2 shows the phase plane in the case where the turbulent Prandtl number, $Pr_t = F/G$ is less than two for all $Ri < Ri_c$. The direction in which the trajectories are travelled can be indicated, since ϕ is positive so that τ increases as t increases. In Fig. 3.3 it is assumed that Pr_t becomes larger than two beyond a certain value of $Ri < Ri_c$.

Both Fig. 3.2 and Fig. 3.3 show that, according to the theory, a decrease in the thickness of the interface is possible only if the initial maximum-slope thickness of the mean velocity profile (y) is relatively large when compared with that of the mean buoyancy profile (x). The mechanism described by Posmentier (1977) then is dominating (see case 2 of Appendix). The phase planes show, however, that the erosion process comes to an end at a certain instant. Afterwards x and, somewhat later, y increase until the

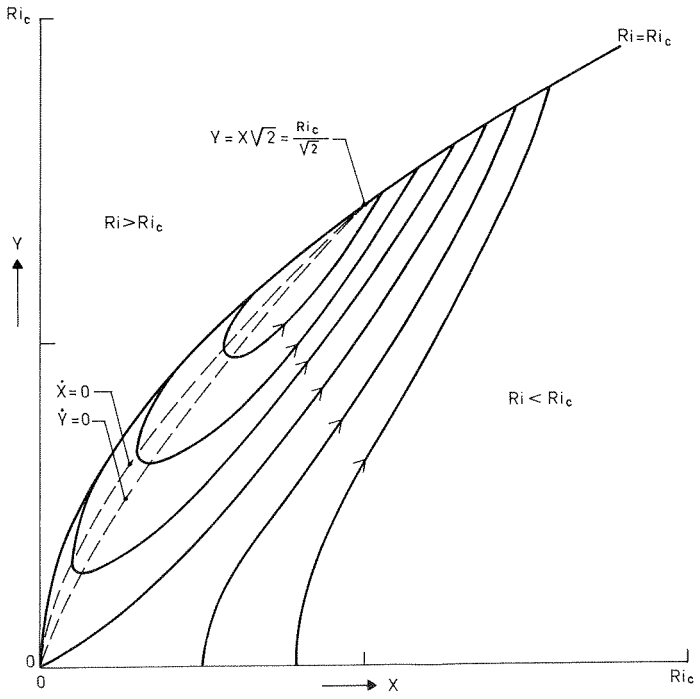

Fig. 3.2 - Schematic of phase plane showing the relationship between y *and* x, $Pr_t < 2$. *The arrows indicate the direction in which the trajectories are travelled as time elapses.*

critical value, Ri_c, of the gradient Richardson number at z=0 is reached. The turbulence then has collapsed and a laminar interface remains. It is notable that this state is reached whatever the initial conditions.

In the case of Fig. 3.2 ($Pr_t < 2$) the final value of the ratio y/x is less than $\sqrt{2}$ indicating that Ri then attains a minimum at z=0 (Eq. 3.5). Collapse of the turbulence then would tend to occur latest at z=0. In free shear flows Pr_t may be larger than two when $Ri \to Ri_c$. Gartrell (1979, Fig. 6.2.41), for instance, plots flux Richardson numbers, Rf, against Ri. His observations suggest that the ratio Ri/Rf is about 2.3 at large Ri, although the

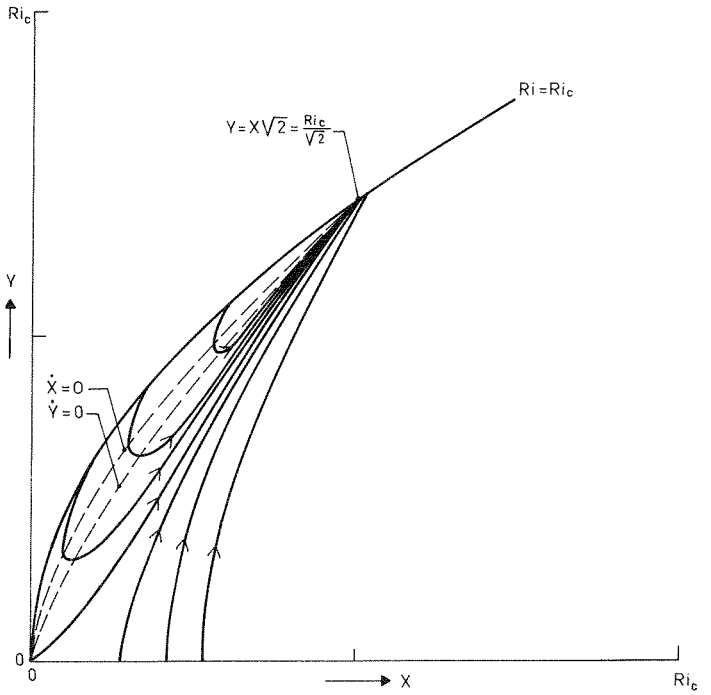

Fig. 3.3 - Schematic of phase plane showing the relationship between y *and* x, $Pr_t > 2$ *when* $Ri \to Ri_c$.

experimental scatter is large. This would indicate that also $Pr_t \simeq 2.3$ at large Ri, also see the comment following (2.22). If $Pr_t > 2$, solutions exist for which y/x goes to $\sqrt{2}$ when Ri tends to Ri_c (Fig. 3.3). Eqs. 3.5 shows that Ri then is approximately independent of z. For small Ri Appendix I gives $y/x \simeq \left[(Pr_t)_{Ri=0}\right]^{\frac{1}{2}}$.

Gartrell (1979, Fig. 6.2.7) observed $y/x \simeq 1$ at $Ri \simeq 0$ up to $y/x \simeq 1.6$ at $Ri \simeq Ri_c$. The critical Richardson number, Ri_c, is given as 0.25 to 0.3; a slight increase in Ri was observed after collapse of the turbulence, however. This value of Ri_c agrees with that observed by Thorpe (1973).

Eqs. 3.13 to 3.15 can be integrated analytically in two special

cases where Pr_t is constant. In one case it is equal to one ($G(Ri) = F(Ri)$), in the other it is equal to two ($G(Ri) = \frac{1}{2} F(Ri)$). These two cases will be discussed briefly.

$Pr_t = 1$

This case would apply to wall-affected turbulence (Arya, 1972). The solution of (3.13) to (3.15) for an initially sharp interface then is

$$y = x = Ri \qquad \text{if} \qquad Pr_t = F/G = 1 \tag{3.17}$$

Eq. 3.13, or 3.14, then becomes

$$\dot{y} + yF'(y) - F(y) = 0 \tag{3.18}$$

If it is assumed, for example, that (Fig. 3.4)

$$F(Ri) = (1 - \frac{Ri}{Ri_c})^2, \qquad 0 < Ri < Ri_c \tag{3.19}$$

the solution of (3.18) becomes

$$y = x = Ri = Ri_c \tanh \frac{\tau}{Ri_c} \tag{3.20}$$

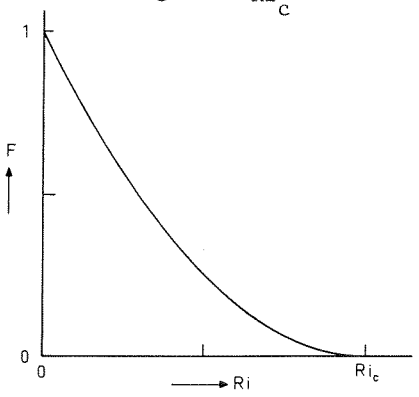

Fig. 3.4 - Function F as given by Eq. 3.19.

$\underline{Pr_t = 2}$

For $Pr_t = 2$ within a certain range of Ri values, a special solution of (3.13) to (3.15) is

$$y = x\sqrt{2} = Ri/\sqrt{2} \qquad \text{if} \qquad Pr_t = F/G = 2 \tag{3.21}$$

At relatively large Ri this solution agrees better with Gartrell's experimental results than (3.17). Eq. 3.13, or 3.14, now becomes

$$\dot{y} - F(y\sqrt{2}) = 0 \tag{3.22}$$

Together with the expression for the function F given by (3.19), (3.22) gives on integration (y(0) = 0)

$$y = x\sqrt{2} = Ri/\sqrt{2} = \frac{\tau\sqrt{2}}{1 + 2\tau/Ri_c} \tag{3.23}$$

The final state ($Ri = Ri_c$) now is approached more gradually.

Fig. 3.5 shows the evolution of Ri as given by (3.20) and (3.23) for $Ri_c = 0.3$, $k = 0.1$ (see Eqs. 3.1 and 3.2) and $\phi = 2$ = constant (see Eqs. 3.3 and 3.4). The assumed value for k is based on observations in a neutrally stratified mixing layer. The value of ϕ is that for tanh-profiles. Fig. 3.5 also shows observations of Gartrell (1979, Fig. 6.2.8). To transform the development as a function of distance (as in Gartrell's experiments) to a development as a function of time, it was assumed that

$$x_1 = \frac{\bar{u}_1 + \bar{u}_2}{2} t$$

where x_1 is the horizontal distance from a boundary, and $\bar{u}_1$ and $\bar{u}_2$ are horizontal velocities in upper and lower layers as defined by Gartrell. Fig. 3.5 indicates a reasonable agreement between theory

and experiments, which, however, is due partly to the particular choice of Ri_c, k and ϕ.

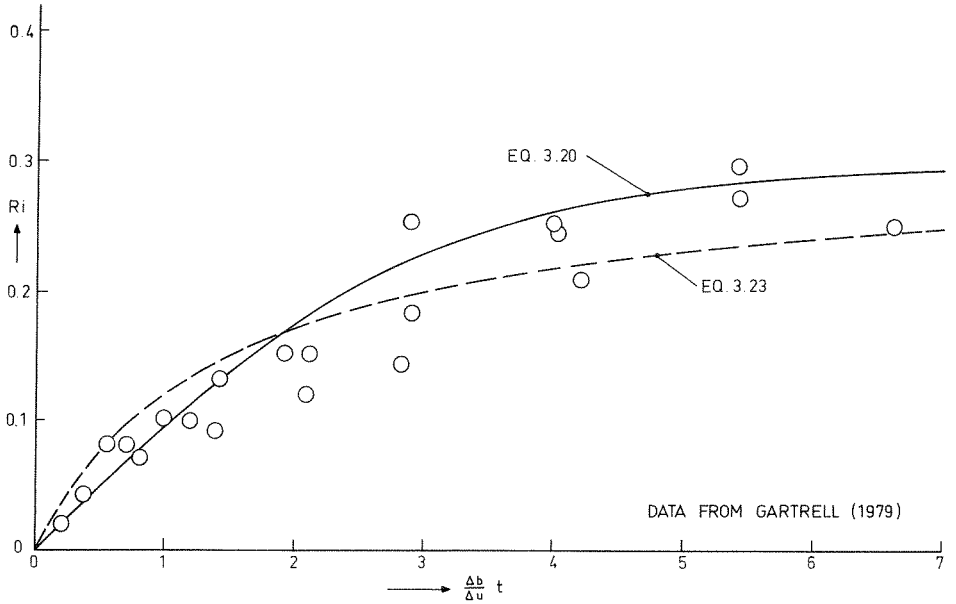

Fig. 3.5 - Evolution of Ri *as a function of time.*

3.3. Discussion

The results of this section differ somewhat from those obtained in section 2 in that, according to the mathematical model examined, erosion of the interface ($\dot{x} < 0$) may occur for certain (rather special) initial conditions. However, the erosion process comes to an end within a finite time interval. Afterwards the thickness of the interface starts to increase. In the final situation, which is approached asymptotically, the Richardson number has become so large that the turbulence collapses. The interface is than thicker than it was initially. Thus a stable behaviour is found again. It may be noted here that persistent erosion may occur in highly inhomogeneous flows where turbulence is continuously produced by a local source. An

example is the development of a mixed layer caused by wind action on a stratified water body. Mellor and Strub (1980), for instance, adopt the gradient-transport concept and show that under certain conditions the velocity and buoyancy profiles remain self-similar during the erosion process. Yet the mean flow then cannot be termed unstable.

The mathematical model seems to correctly describe, at least qualitatively, the overall features of a developing mixing layer at an initially sharp interface. This may be a somewhat unexpected result in particular so far as the initial phase is concerned, since the rolling up of the vortex layer related to the Kelvin-Helmholtz instability mechanism produces well-defined structures (billows). If the homogeneous layers are laminar, turbulence does not come about until the billows break. Apparently, exact knowledge about the structures of the flow is not necessary in the case considered to predict mean-flow quantities. For quantitative agreement, however, mathematical models of the type examined have the well-known drawback that tuning to experimental results by introducing adjustable constants is unavoidable.

4. CONCLUSIONS

Some qualitative properties of a relatively simple gradient transport model for turbulent, stratified flow were analyzed. Particular attention was devoted to the dynamical stability of statically stable flow. It was found that shear flow is likely to be stable, since stability conditions 2.21 and 2.22 seem to be satisfied in real flows. This result contradicts certain suggestions found in the literature, also see Linden (1979) and McEwan (1980). Moreover a more fundamental objection against instability concerning mean-flow variables can be raised (section 2.3).

In a flow which is stable in the sense examined herein, sharp interfaces will not develop spontaneously if the turbulence is homogeneous. It was shown in section 3 that an interface between two homogeneous layers may tend to sharpen for rather special initial conditions. The process is only temporary, however. The interface starts to thicken after a finite time interval, and finally the turbulence collapses. Certain results for a developing mixing layer are in reasonable agreement with the experiments of Gartrell (1979).

The relevance of the gradient-transport concept from a physical point of view was not discussed. Woods (1977), for instance, gives an account of the objections to this concept in the case of stratified flow in the ocean.

REFERENCES

Arya, S.P.S., 1972: The critical condition for the maintenance of turbulence in stratified flows. *Quart. J. Roy. Meteorol. Soc.*, 98, 264-273.

Gartrell, Jr., G., 1979: *Studies on the mixing in a density stratified shear flow.* W.M. Keck Lab. of Hydr. and Water Res., California Institute of Technology. Report No. KH-R-39.

Kranenburg, C., 1980: On the stability of turbulent density-stratified shear flow. *J. Phys. Oceanogr.*, 10, 1131-1133.

McEwan, A.D., 1980: Mass and momentum diffusion in internal breaking events. In: *Proc. Second Int. Symp. on Stratified Flows*, 2, T. Carstens and Th. McClimans (eds.), Tapir Press, Trondheim.

Mellor, G.L. and P.T. Strub, 1980: Similarity solutions for the stratified turbulent Rayleigh problem. *J. Phys. Oceanogr.*, 10, 455-460.

Phillips, O.M., 1972: Turbulence in a strongly stratified fluid - is it unstable? *Deep-Sea Res.*, 19, 79-81.

Posmentier, E.S., 1977: Tne generation of salinity finestructure by vertical diffusion, *J. Phys. Oceanogr.*, 7, 298-300.

Sherman, F.S., J. Imberger and G.M. Corcos, 1978: Turbulence and mixing in stably stratified waters. *Ann. Rev. Fluid Mech.*, 10, 267-288.

Thorpe, S.A., 1971: Experiments on the stability of stratified shear flows: miscible fluids. *J. Fluid Mech.*, 46, 299-319.

Thorpe, S.A., 1973: Experiments on instability and turbulence in a stratified shear flow. *J. Fluid Mech.*, 61, 731-751.

Townsend, A.A., 1976: *The Structure of Turbulent Shear Flow*. 2nd ed. Cambridge University Press.

Turner, J.S., 1973: *Buoyancy Effects in Fluids*. Cambridge University Press.

Walters, R.A., G.F. Carey and D.F. Winter, 1978: Temperature computation for temperate lakes. *Appl. Math. Modelling*, 2, 41-48.

Webster, C.A.G., 1964: An experimental study of turbulence in a density-stratified shear flow. *J. Fluid Mech.*, 19, 221-245.

Woods, J.D., 1977: Parameterization of Unresolved Motions. In: *Modelling and Prediction of the Upper Layers of the Ocean*, E.B. Kraus (ed.), Pergamon Press, 118-142.

NOTATION

b	buoyancy
F,G	functions representing the damping caused by stratification
g	acceleration due to gravity
h	depth of layer
k	wave number, constant
K	diffusivity matrix
K_m, K_b	eddy viscosity and eddy diffusivity
l	mixing length
N	buoyancy frequency
Pr_t	turbulent Prandtl number
Ri	gradient Richardson number
Ri_c	critical value of Ri
t	time variable
u_*	shear velocity
x,y	dimensionless maximum-slope thicknesses of buoyancy and velocity profiles
z	vertical coordinate, positive in upward direction
α, β	constants
Δu, Δb	velocity and buoyancy differences
δ_u, δ_b	maximum-slope thicknesses of velocity and buoyancy profiles
λ	frequency
ρ	density
τ	dimensionless time variable
ϕ	time function
$..{}_n$	neutral conditions
$..{}_o$	undisturbed situation, value at z=0
$\overline{..}$	mean value
$..'$	differentiation

APPENDIX - ANALYSIS OF EQUATIONS 3.13 TO 3.15

The phase planes in Figs. 3.2 and 3.3 representing the solution of Eqs. 3.13 to 3.15, are based on the analysis of the following special cases.

1. The case where Ri is small

Eqs. 3.13 and 3.14 become

$$\dot{y} - F(0) \simeq 0$$

$$\dot{x} - \frac{y}{x} G(0) \simeq 0$$

Integrating these equations gives

$$y(\tau) = y(0) + F(0)\tau \tag{A.1}$$

$$x(\tau) = \left[x(0)^2 + 2y(0)\, G(0)\tau + F(0)\, G(0)\, \tau^2\right]^{\frac{1}{2}} \tag{A.2}$$

Eqs. A.1 and A.2 show that the gradient Richardson number, $Ri = y^2/x$, increases with time when τ is sufficiently large. Consequently, (A.1) and (A.2) do no longer hold good after a certain initial period.

If $x(0) = y(0) = 0$ (initially sharp interface), (A.1) and (A.2) give

$$\frac{y}{x} = \left[\frac{F(0)}{G(0)}\right]^{\frac{1}{2}} = \left[(Pr_t)_{Ri=0}\right]^{\frac{1}{2}} \tag{A.3}$$

2. The case where $y >> x$

Neglecting in (3.14) the term $2/y^2$ with respect to $1/x^2$ gives

$$\dot{x} \simeq \frac{y}{x} (RiG' + G) = \frac{y}{x} (RiG)' \qquad (A.4)$$

which is equivalent to Posmentier's (1977) criterion: erosion ($\dot{x} < 0$) occurs if $(RiG)' < 0$. The time derivative of Ri becomes, with the same neglect in (3.13),

$$\dot{Ri} = Ri(2 \frac{\dot{y}}{y} - \frac{\dot{x}}{y}) \simeq - Ri \frac{y}{x^2} (RiG' + G - 2RiF' - 2 \frac{x^2}{y^2} F) \qquad (A.5)$$

The last term in (A.5) is negligible, since $y >> x$. This equation may then be written as

$$\frac{\dot{Ri}}{Ri} \simeq - \frac{y}{x^2} \left[F \frac{d}{dRi} (Ri \frac{G}{F}) + (2 - \frac{G}{F})(- RiF') \right] \qquad (A.6)$$

The inequalities 2.22 and 2.23 indicate that $\dot{Ri}$ is negative. This result implies that if $(RiG)'$ and $\dot{x}$ are negative, they are temporary so, since $(RiG)'$ in Eq. A.4 becomes positive at smaller values of Ri.

3. The case where $y \leqq x\sqrt{2}$

Eqs. 3.13 and 3.14 show that both $\dot{y}$ and $\dot{x}$ are positive if $y \leqq x\sqrt{2}$. If $y = x\sqrt{2}$ at a certain instant, then

$$\frac{\dot{y}}{\dot{x}} = \frac{dy}{dx} = \frac{x}{y} \frac{F}{G} = \frac{Pr_t}{\sqrt{2}} \qquad \text{if} \qquad \frac{y}{x} = \sqrt{2} \qquad (A.7)$$

The slope of a trajectory in the phase plane is less (greater) than $\sqrt{2}$, if $Pr_t < 2$ (>2).

4. The case where $\dot{y} = 0$ at a certain instant

Eq. 3.13 gives with $\dot{y} = 0$

$$(\frac{y}{x})^2 = 2 + \frac{F}{(-RiF')} \tag{A.8}$$

Eq. A.8 shows that $y/x > \sqrt{2}$. For a large class of functions, F tends more rapid to zero than its first derivative when $Ri \to Ri_c$. In that case $\dot{y} = 0$ at $y/x \to 2$ when $Ri \to Ri_c$.

Eqs. A.8 and 3.14 give, after some manipulation,

$$\frac{\dot{x}}{x} = \frac{1}{y} \frac{F^3}{(-RiF')} \frac{d}{dRi} (Ri \frac{G}{F^2}) \tag{A.9}$$

According to (2.23) $\dot{x}$ is positive. A steady-state situation ($\dot{x} = \dot{y} = 0$) therefore does not exist when $Ri < Ri_c$. Since

$$\frac{\dot{Ri}}{Ri} = 2 \frac{\dot{y}}{y} - \frac{\dot{x}}{x} = - \frac{\dot{x}}{x} \tag{A.10}$$

the time derivative of Ri is negative.

5. The case where $\dot{x} = 0$ at a certain instant

Eq. 3.14 gives with $\dot{x} = 0$

$$(\frac{y}{x})^2 = \frac{2RiG'}{G+RiG'} = \frac{2RiG'}{(RiG)'} = 2 + \frac{2G}{-(RiG)'} \tag{A.11}$$

Eq. A.11 shows that $\dot{x}$ can be zero only if $(RiG)' < 0$, consequently at relatively large Ri. In that case $y/x > \sqrt{2}$, and $y/x \to \sqrt{2}$, when $Ri \to Ri_c$ for the class of functions mentioned in case 4. Eqs. A.11 and 3.13 give

$$\dot{y} = \frac{F^3}{(RiG)'} \frac{d}{dRi} (Ri \frac{G}{F^2}) \tag{A.12}$$

Inequality 2.23 and the fact that $(RiG)' < 0$ in this case show that $\dot{y}$ is negative. As a consequence, $\dot{Ri}$ is also negative.